An Alternative Method for Measurement of Radiated Emissions According to CISPR 25

Jin Jia, Denis Rinas, Stephan Frei
TU Dortmund University
Dortmund, Germany
jin.jia@tu-dortmund.de
denis.rinas@tu-dortmund.de
stephan.frei@tu-dortmund.de

Abstract—**Current scanning methods could be a promising alternative to reduce the need of automotive CISPR 25 ALSE measurements. It is assumed that, especially in low frequency range, the cable bundle is often the dominant radiating structure. Knowing the current distribution along the cable bundle the field at any point can be calculated. First implementation calculated the phase through measured current amplitude, which may produce the error in low frequency range. In order to compensate the mentioned problem, this paper proposes two alternative enhancements of the common-mode current scan methods in time domain for cable bundles. A time domain scan can provide the amplitude and phase information of currents simultaneously through Fast Fourier Transform (FFT). One method, considering the common-mode current as radiation source, models the cable bundle by a set of elementary dipoles to calculate the field emissions. While the other method only uses common-mode current and transmission line parameters at beginning and end ports of cable bundle to calculate the field emissions. Till now an ideal environment was assumed and the complexity of a real ALSE was neglected. In order to improve the prediction quality, a calibration approach based on measured data is proposed, which incorporates real influence factors in an anechoic shielded chamber. Through the verifications by numerical analysis of different cable bundle models and measurements, the stability and feasibility of the mentioned improvements could be shown.**

Keywords-Automotive CISPR 25; FFT; cable bundle; common-mode current; radiated emission; calibration

I. INTRODUCTION

In the development of new electronic products, radiated emissions must be analyzed. For automotive systems the ALSE method from CISPR 25 [1] is often applied. Fields from components or modules connected to a cable bundle are measured in an anechoic shielded chamber, which is expensive and space consuming. Therefore it is desired to find new alternative test methods. Because in many cases the common-mode current from cable bundles dominates the radiated emissions [2], the measurements of the currents and processing of the data could be a promising alternative. For obtaining the current distribution along a cable bundle, RF current probe is adopted in a near field scan system, which can be connected to voltage measurement devices (oscilloscope, spectrum analyzer or receiver), as shown in figure 1.
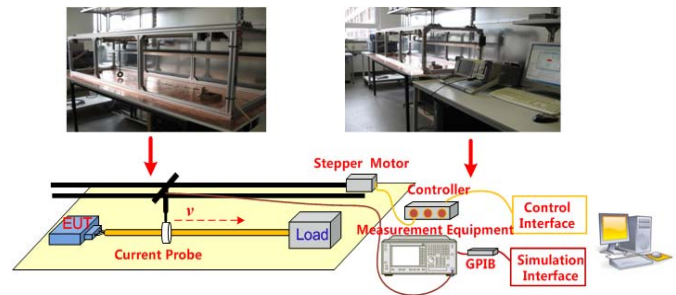

Figure 1. Measurement system for common-mode current distribution

Amplitude and phase of the common-mode current distribution are both necessary in an accurate radiation model for prediction of far-fields from a cable bundle. In a previous paper [3] a current amplitude scanning method in frequency domain (CASM-FD) was proposed to predict radiated emissions from a cable bundle. The phase is retrieved based on the measured current amplitude distribution. This method can evaluate well the field emissions above 30 MHz up to minimum 1 GHz successfully through a calculated phase distribution. Furthermore the EMC test receiver used in CASM-FD can guarantee high amplitude resolution and signal-to-noise-ratio (SNR). However due to the problems with predicting radiated emissions in low frequency range, improvements are needed to compensate this weakness of CASM-FD. A time domain scan method [4], which derives amplitude and phase in frequency domain of a spatial current distribution simultaneously through FFT, could overcome the problems in a wider frequency range. This paper provides two time-domain scanning methods to predict radiated emissions from a cable bundle. Current scanning method in time domain (CSM-TD) acquires the common-mode current along the entire cable bundle. While the other method only requires measured common-mode current at the beginning and end of a cable bundle (two-port current method, TPCM) and common-mode parameters of the cable bundle. Therefore CASM-FD, CSM-TD and TPCM constitute a set of approaches to predict field emissions from cable bundle based on common-mode current scan, as shown in figure 2.

The goal of proposed methods is to substitute at least for pre-compliance-tests the expensive radiated-emission tests in anechoic shielded chambers. To reach better acceptance the

real environment, e.g. reflections due to imperfect absorbing materials or antenna effects, has to be characterized and methods for taking the environmental effects into account are required. Even very complex numeric simulation models cannot reflect the real test configuration in chamber nowadays, which may exert a great influence to the received antenna voltage [5]. Therefore a calibration method based on measured data in a real anechoic shielded chamber is presented in this work to predict the real field emissions from a current scan.
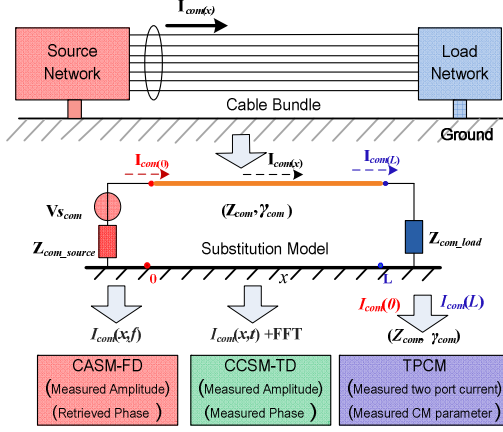

Figure 2. Alternative methods based on common-mode current scan

II. COMMON-MODE CURRENT SCAN METHODS

The CASM-FD (Current Amplitude Scanning Method in Frequency Domain) can retrieve phase information based on measured current amplitude distribution [3]. However the overall accuracy of CASM-FD mainly depends on accuracy of the retrieved phase and it especially fails to predict the field emissions in low frequency range. Furthermore this method needs an iteration algorithm at each frequency in the considered frequency range, which may require much computation. Therefore this section presents two measurement methods which help to predict more accurately the radiated fields: CSM-TD and TPCM.

A. Current scanning method in time domain (CSM-TD)

CSM-TD can be realized using a two-channel oscilloscope. For obtaining desired amplitude and phase information simultaneously, the measured data is transferred to frequency-domain results via FFT. In order to obtain correct current phase information along a cable bundle, a reference signal is necessary. Voltage or current at the start point of a cable bundle can be used as reference signal for triggering the oscilloscope. Then current probe is connected to a second channel to scan the nodes along the cable bundle: [1, 2,···, N], as shown in figure 3. The current phase at the reference node and scanned nodes can be obtained simultaneously via FFT, and then the relative phases at the scanned nodes can be calculated according to:

$$Node\ I^{th} : [\varphi_1 + \Delta\varphi_c] - [\varphi_0 + \Delta\varphi_r] = [\varphi_1 - \varphi_0] + [\Delta\varphi_c - \Delta\varphi_r]$$
$$Node\ 2^{th} : [\varphi_2 + \Delta\varphi_c] - [\varphi_0 + \Delta\varphi_r] = [\varphi_2 - \varphi_0] + [\Delta\varphi_c - \Delta\varphi_r]$$
$$\vdots \qquad\qquad\qquad \vdots \qquad\qquad (1)$$
$$Node\ N^{th} : [\varphi_N + \Delta\varphi_c] - [\varphi_0 + \Delta\varphi_r] = [\varphi_N - \varphi_0] + [\Delta\varphi_c - \Delta\varphi_r]$$

Here φ_N is the phase at node N^{th}, φ_0 is the phase of the reference signal, $\Delta\varphi_r$ and $\Delta\varphi_c$ are phase shifts induced by connecting coaxial cables from reference probe and current probe to oscilloscope respectively. For deleting these phase shifts, the phases at all the nodes are normalized to the end node of the cable bundle according to (2):

$$Node\ I^{th} - Node\ N^{th} : [\varphi_1 - \varphi_N]$$
$$Node\ 2^{th} - Node\ N^{th} : [\varphi_2 - \varphi_N]$$
$$\vdots \qquad\qquad (2)$$
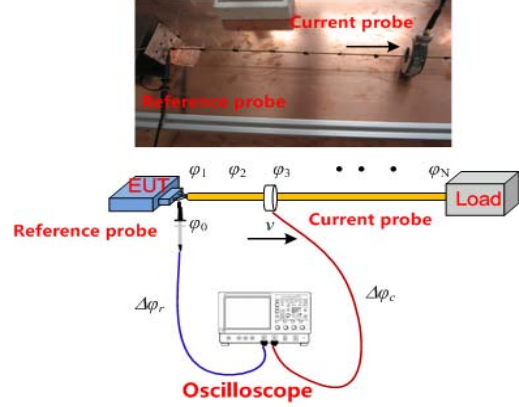$$Node\ N^{th} - Node\ N^{th} : 0$$

Figure 3. Measurement configuration for CSM-TD

B. Two- port current method(TPCM)

Using an analytic radiation model of a transmission line [6-7], measurements of common-mode voltages and currents at the beginning and end port of a cable bundle can be sufficient to calculate the radiated field. However, due to problems with common-mode voltage measurement, the voltages can be derived from two-port currents and ABCD transmission line matrix according to:

$$\begin{bmatrix} U_{com}(0) \\ U_{com}(L) \end{bmatrix} = \begin{bmatrix} \dfrac{A}{C} & B - \dfrac{AD}{C} \\ \dfrac{1}{C} & -\dfrac{D}{C} \end{bmatrix} \begin{bmatrix} I_{com}(0) \\ I_{com}(L) \end{bmatrix} \qquad (3)$$

ABCD matrix of a cable bundle is a mathematic model to describe port quantities of a two-port network, which can be calculated by measured common-mode S-parameters from network analyzer:

$$\begin{bmatrix} A & B \\ C & D \end{bmatrix} = \begin{bmatrix} \dfrac{(1+S_{11})(1-S_{22}) + S_{12}S_{21}}{2S_{21}} & Z_n \dfrac{(1+S_{11})(1+S_{22}) - S_{12}S_{21}}{2S_{21}} \\ Z_n \dfrac{(1-S_{11})(1-S_{22}) - S_{12}S_{21}}{2S_{21}} & \dfrac{(1-S_{11})(1+S_{22}) + S_{12}S_{21}}{2S_{21}} \end{bmatrix} \qquad (4)$$

Here Z_n is the port reference impedance of network analyzer (50 Ω). In a similar manner like in CSM-TD, oscilloscope is used to acquire the common-mode currents at the beginning and end ports of the cable bundle. Then FFT computes the amplitude and phase of currents. Other than requiring currents at N nodes of the entire cable bundle in CSM-TD, TPCM only needs the current information at beginning and end node and the ABCD parameter matrix, as shown in figure 4. But compared to CSM-TD, TPCM needs to measure common-

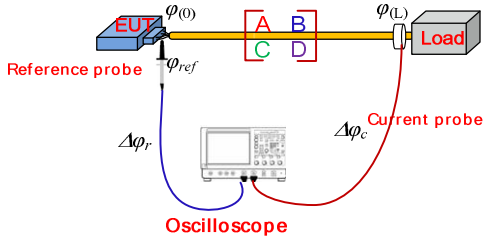mode transmission line parameters of cable bundle which means an application limitation in real testing.

Figure 4. Measurement configuration for TPCM

III. RADIATION MODELS FOR CABLE BUNDLES

A cable bundle in automotive application commonly carrying tightly packed insulated wires, thus it is reasonable to neglect the cross section distribution and the contribution of differential mode currents to radiated emissions. Therefore a radiation model of a cable bundle can be simplified to a single transmission line, which only considers common-mode current path, as shown in figure 2.

Since common-mode current acts as the main radiation source from a cable bundle, the manner how a current distribution is acquired, gives different prediction models. The CASM-FD scans the current amplitude in frequency domain and then retrieves the phase information from the amplitude distribution. The CSM-TD scans in time domain and uses FFT algorithm to obtain current amplitude and phase distribution simultaneously. Both methods adopt multi-dipole model to calculate the radiation, which divides the common-mode current path into a set of short segments represented by radiating dipoles [3]. While substituting the scanned current along the entire cable, the TPCM requires common-mode current and parameters at the beginning and end port of a cable bundle. This method uses an analytic model of a radiating cable to predict the fields [6]. It must be noted that the analytic model is only available when the common-mode velocity v_{com} of the current is the same as the electromagnetic wave propagation velocity c_0 in free space [7]. However v_{com} of automotive cable bundles in practical application is less than c_0 due to dielectric coating. At lower frequencies it can be assumed that v_{com} is approximately c_0.

IV. CONSIDERING THE ALSE ENVIRONMENT BY CALIBRATION

According to CISPR 25, the ALSE method must be implemented in an anechoic shielded chamber with specific EMC test antenna. For example an active rod antenna is used to measure radiated disturbance below 30 MHz; a compact bilog antenna (CBL) measures radiated emissions from 30 MHz to 1 GHz, as shown in figure 5.

In the proposed methods (CASM-FD, CSM-TD or TPCM), the metallic table in figure 5 can be approximated by an infinite ground through mirror theory or more accurate PO-model (physical optics). The PO-model replaces the finite metallic table by equivalent surface current according to PO

method [6]. However the ideal simulation models are problematic due to the complex behavior of the anechoic chamber, where edge current and reflection from chamber walls influence the antenna received voltage. Therefore it is necessary to take these factors into account. Measurement-based approaches are more promising. In calibration process, a 1.5 m long single wire, fed by sinusoidal signal at several frequencies point, was used to obtain correction data according to:

$$K_{cal} = E_{CASM-FD/CSM-TD/TPCM} - E_{antenna}$$
$$E_{antenna} = V_{antenna} + AF_{antenna}$$

(5)

Where $E_{antenna}$ is the measured electric field of test antenna at reference point in anechoic shielded chamber, $E_{CASM\text{-}FD/CSM\text{-}TD/TPCM}$ are calculated value through CASM-FD, CSM-TD or TPCM based on measured current data of the single wire. Correction factors are fingerprints of a test chamber and will vary from location to location. Therefore this calibration method should be applied in each test chamber to predict electric field. It can be furthermore a very useful method to compare different test chambers.
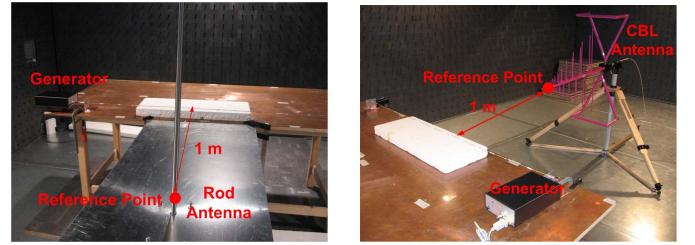

Figure 5. Configurations with the active rod and CBL antenna for measurement of the correction factors

A. Active rod antenna measurement below 30 MHz

In correct standard test configuration of an active rod antenna as shown in figure 5 (left), the frequency response below 30 MHz should be a straight line. However due to capacitive coupling between metallic table and chamber ground, one or more resonances in a measured curve may be observed. For example in figure 6, the resonance occurs around 2 MHz when metallic table is disconnected to chamber ground (Measurement 2); while the resonance is shifted to 15 MHz when metallic table is connected to ground (Measurement 1). The cable was also placed on the chamber ground to remove capacitance coupling. Resonances cannot be observed any more (Measurement 3). Some measures could suppress the resonances in table configuration to improve the test accuracy [8].

Based on the measured current amplitude and phase along the cable from Network Analyzer and the mirror theory, the calculated results from multi-dipole method can match well with MoM and Measurement 3, as shown in figure 6. Therefore the dipole model and an infinite ground model can provide enough calculation accuracy compared to real active rod antenna test results, when the resonance effect in measurement can be suppressed. However the proposed alternative methods are only to calculate the vertical electric field at reference point, while the rod antenna test obtains

antenna voltage first and then adds the antenna factor (AF) from manufacturer. For getting the same radiated emissions as ALSE method through alternative approaches, the correction factor could be also necessary to determine the position of reference point.
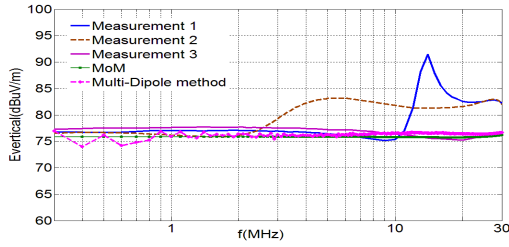

Figure 6. Measured and simulated data by calibration below 30 MHz of an active rod antenna test

B. CBL antenna measurement from 30 MHz to 1 GHz

In real CBL antenna measurement as shown in figure 5 (right), the infinite ground model through mirror theory cannot simulate the influence from metallic table, especially in horizontal polarization. Figure 7 depicts electric field data at reference point of CBL antenna in vertical direction from MoM or CASM-FD/CSM-TD (only results from CASM-FD are presented). It can be seen that both PO-model and infinite ground model applied in CASM-FD can simulate vertical electric field well. The E-field from infinite ground model is nearly 6 dB higher than the field from PO-model from 30 MHz to 1 GHz, which mainly originates from edge current of metallic table. Compared to vertical component, the horizontal component is more sensitive to the influence of edge current on the metallic table, as shown in figure 8. From the simulation of MoM and CASM-FD, the results from finite ground are nearly 25 dB higher than from infinite ground. Compared to MoM, the PO-model applied in alternative methods can also improve the prediction accuracy.
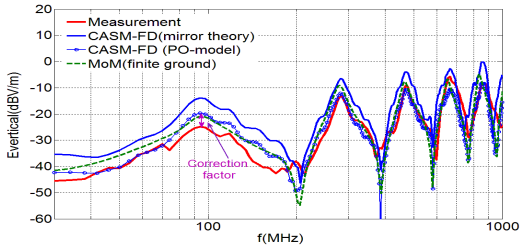

Figure 7. Measured and simulated data by calibration in vertical direction from 30 MHz to 1GHz of a CBL antenna test
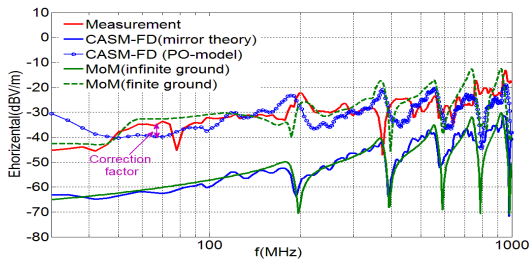

Figure 8. Measured and simulated data for calibration in horizontal direction from 30 MHz to 1GHz of a CBL antenna test

V. METHOD VERIFICATION

A. A simple configuration setup with a single cable

In order to verify the proposed TPCM which needs currents and voltages at beginning and end ports of cable bundle, the radiation from a single cable driven by a pulse of 100 kHz and 2.5 V-amplitude was investigated. For guarantying the correctness of measurement as reference, the cable and rod antenna are placed on chamber ground to remove resonance from capacitive coupling depicted in figure 6. The radiation test configuration is shown in figure 9. The active 1 m-rod antenna is used to measure the vertical electric field. The calculated results from CSM-TD, TPCM and CASM-FD are depicted in figure 10. The curves from CSM-TD and TPCM almost coincide. They both match well with measurement. While the curve obtained from CASM-FD with a calculated phase distribution shows larger deviation around 1.5 MHz.
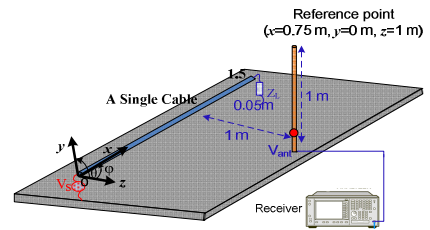

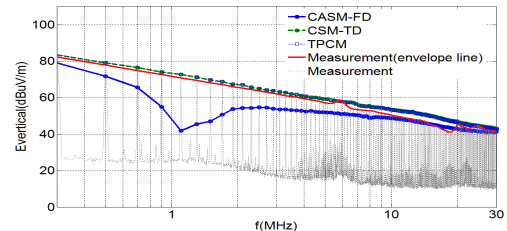Figure 9. Analyzed configuration of a single cable

Figure 10. E-field at observation point below 30 MHz

B. A complex configuration setup with a seven-cable bundle

The proposed CASM-FD/CSM-TD and calibration method are also applied to predict vertical and horizontal electric field from a seven-cable bundle, which is terminated randomly with resistors as shown in figure 11. The fed cable was driven by a 3.3 V- trapezoidal pulse signal with repetition frequency of 40 MHz.
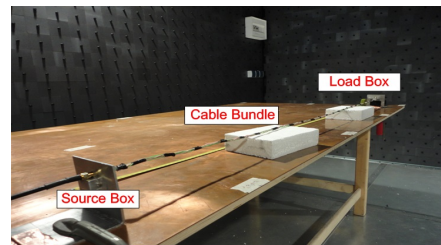

Figure 11. Analyzed configuration of a seven-cable bundle

The comparisons between CASM-FD/CSM-TD and measurement of vertical and horizontal electrical field at reference point of CBL antenna are presented in figure 12 and

13 respectively. Figure 14 depicts the bar charts of deviation from CASM-FD/CSM-TD in vertical and horizontal components compared to measurement. In vertical polarization, the deviations from CASM-FD can be reduced to less than 4 dB. The average error of all the harmonics peaks is 1.95 dB. Deviation from CSM-TD can be in 5 dB except 360 MHz. And the average error of all the harmonics peaks is 3.08 dB. Compare to vertical component, the calculation results in horizontal direction show higher deviation due to the instability of measured data in calibration process. The average errors of CASM-FD and CSM-TD are 5.2 dB and 3.96 dB respectively. The maximal deviation nearly amounts to 13 dB at 280MHz and 480 MHz. it can be observed that these two frequency points locate around resonance range in horizontal calibration curve of figure 8, at which the horizontal field measured by CBL antenna is very sensitive to test configuration.
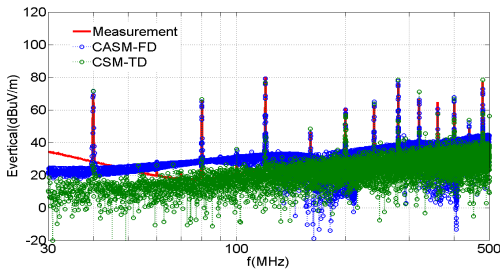

Figure 12. Vertical E-field by measurement and CASM-FD/ CSM-TD
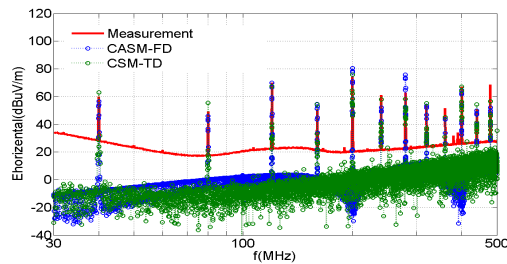

Figure 13. Horizontal E-field by measurement and CASM-FD/ CSM-TD
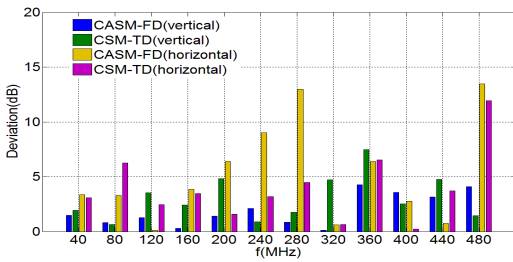

Figure 14. Deviation distribution of CASM-FD/CSM-TD compared to Measurement in vertical and horizontal polarization

C. A configuration setup with stepper motor driver

In above verifications the signal is a simple pulse. Real disturbances from electronics are more complex. Therefore the proposed alternative methods were also applied to predict the radiated emissions from a stepper motor with a processor control system. Figure 15 shows the radiation test configuration above 30 MHz in an anechoic chamber. The measured results are used as the reference to evaluate the CASM-FD and CSM-TD.
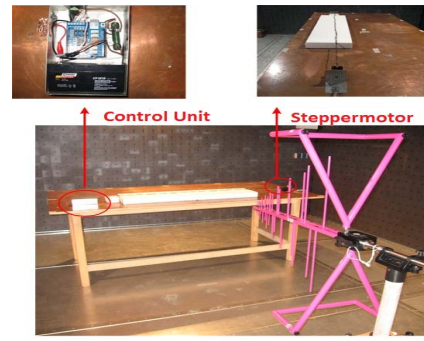

Figure 15. Analyzed configuration of stepper motor system above 30 MHz

Figure 16 and 17 present the predicted fields and measurement from the CBL antenna in vertical and horizontal polarization respectively. In general the results in vertical direction from CASM-FD and CSM-TD both predict many of the measured peaks well, but in some cases the deviation exceeds 3 dB. The error over frequency is shown for the peaks in figure 18 (upper). The average errors from CASM-FD and CSM-TD are 2.49 dB and 2.35 dB respectively. At main harmonics peaks which exceeding the limit of average class-5 (64 MHz, 96 MHz, 128 MHz, 288 MHz and 384 MHz), the errors from CASM-FD amount to 0.58 dB, 0.61 dB, 0.96 dB, 1.67 dB and 5.85 dB; while errors from CSM-TD are 1.12 dB, 3.1 dB, 1.53 dB, 1.72 dB and 1.98 dB. Compared to vertical polarization, the horizontal emission includes less radiated peaks. Figure 18 (lower) shows the error over frequency for the harmonic peaks for horizontal polarization. The average errors from CASM-FD and CSM-TD are 2.34 dB and 3.4 dB respectively. The limit-exceeding peaks (32 MHz, 64 MHz, 128 MHz, 192 MHz, 288 MHz and 384 MHz), show errors with CASM-FD of 0.08 dB, 0.38 dB, 3.71 dB, 4.49 dB, 6.45 dB, 1.07 dB; while errors from CSM-TD amount to 5.03 dB, 2.47 dB, 3.46 dB, 1.11 dB, 3.81 dB and 0.46 dB.
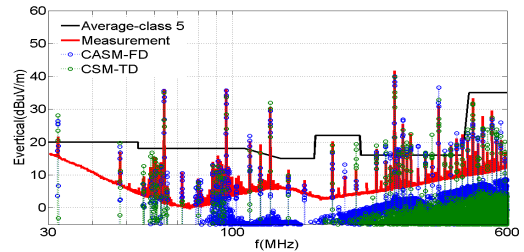

Figure 16. Vertical E-field from stepper-motor system by measurement and CASM-FD/CSM-TD above 30 MHz
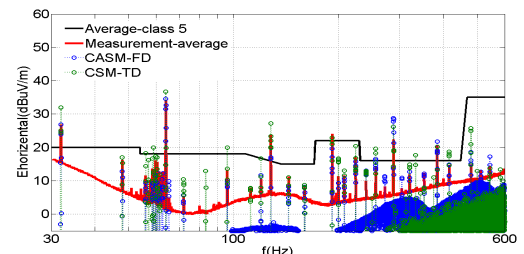

Figure 17. Horizontal E-field from stepper-motor system by measurement and CASM-FD/ CSM-TD above 30 MHz
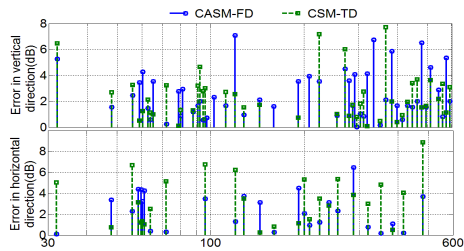
Figure 18. Error from CASM-FD/CSM-TD in vertical/horizontal direction

Except the prediction of radiated emission above 30 MHz, also investigated radiated emission from the stepper motor system in low frequency range was investigated. Configuration 2 (figure 19 (right)) shows the rod antenna test setup according to ALSE method in CISPR 25. However, capacitive coupling from metallic table to chamber ground is a well known problem of this method and leads to resonances in measurements. Therefore configuration 1 where equipment under test was placed directly on the floor of the ALSE (figure 19 (left)) was chosen to provide a better measured reference to evaluate alternative approaches.
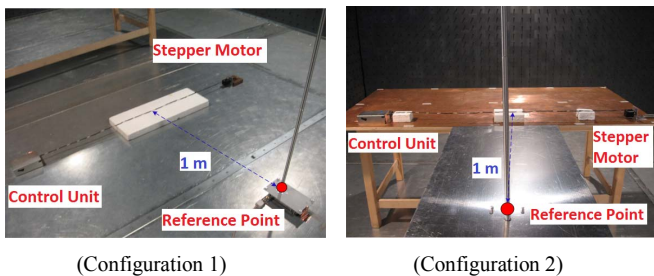

(Configuration 1)   (Configuration 2)

Figure 19. Analyzed configurations of stepper motor in low frequency range

Figure 20 depicts the vertical E-filed at reference point of rod antenna from direct measurement and CSM-TD. An apparent deviation (Error 2) can be seen between measurements of configuration 2 and configuration 1, which originating from the capacitive coupling in configuration 2. Compared to measurement of configuration 1, the proposed CSM-TD can acquire accurate prediction result at main peaks of 16 MHz, 32 MHz and 48 MHz. The errors are 1.89 dB, 1.34 dB and 1.45 dB respectively. However CSM-TD fails to predict the fields below 5 MHz, in which the maximal deviation (Error 1) could reach nearly 10 dB. The main reason for this deviation is not known yet. Instability of trigger conditions may be a reason.
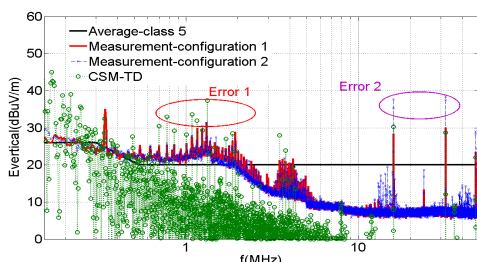

Figure 20. Vertical E-field from stepper-motor system by measurement and CSM-TD in low frequency rang

VI. CONCLUSION

This work shows that CASM-FD [3] can be modified in order to overcome the low-frequency phase calculation problems. Two methods were proposed. The CSM-TD uses time domain current measurements, and then applies FFT algorithm to find spatial amplitude and phase distribution along a cable bundle. The other method TPCM needs only the common-mode currents and S-parameters at two endings of a cable. Furthermore in order to incorporate the real influence factors of measurement in an anechoic shielded chamber, a calibration method based on measured data was proposed. The correction factor can effectively improve prediction accuracy both in vertical and horizontal polarization.

Through the verifications of a single cable, TPCM seems to be accurate in low frequency range. Because CSM-TD can acquire real phase distribution, it is also an effective alternative to prediction field emissions in low frequency range. The deficiencies of CASM-FD in low frequency range can be overcome by these two approaches. More complicate configuration of a seven-cable bundle and stepper motor system was investigated to verify CASM-FD/CSM-TD and proposed calibration method. Both methods can reach good prediction accuracy as a pre-compliance test. However the radiated emission levels can be very low in real EMC configuration, which could be a big challenge for the application of proposed alternative methods. Therefore further investigations are necessary, about how to improve the acquisition accuracy of current data especially in time domain and the reliability of correction data especially in horizontal polarization.

REFERENCES

[1] CISPR 25 Ed.3, "Vehicles, boats and internal combustion engines-Radio disturbance characteristics – Limits and methods of measurements for the protection of on-board receivers", 2007.

[2] J. Q. Wang, O. Fujiwara, K. Sasabe, "A simple method for predicting common-mode radiation from a cable attached to a conducting enclosure," APMC 2001, Dec. 2001, Vol: 3, pp.3-6.

[3] J. Jia, D. Rinas, S. Frei, "Prediction of radiated fields from cable bundles based on current distribution measurements", EMC Europe 2012, Rome, Sept. 2012, pp. 1-7.

[4] D. Rinas, S. Niedzwiedz, J. Jia, S. Frei, "Optimization methods for equivalent source identification and electromagnetic model creation based on near-field measurements", EMC Europe 2011, York, Sept. 2011, pp. 298-303.

[5] F. J. Bongartz, J. Deckers, M. Heina, "Proposal for the validation of absorber lined shield enclosure for CISPR 25 emissions tests", IEEE International Symposium on Electromagnetic Compatibility, pp. 116-120, Aug. 2009.

[6] J. Jia, F. Kremer, S. Frei, "Modellierung von CISPR-25 Antennenmessungen mittels schneller approximierender Berechnungsverfahren", EMV-Düsseldorf, Germany, 2012.

[7] J. Jia, S. Frei, "Analysis of radiated emissions from flexray automotive bus system", EMC Europe 2011, York, Sept. 2011, pp. 234-239.

[8] D. Warkentin, A. Wang, W. Crunkhorn, "Shield Enclosure Accuracy improvements for MIL-STD-461E Radiated Emission Measurement", IEEE International Symposium on EMC, August 2005 in Chicago, USA.